The nucleoporin Nup98 associates with the intranuclear filamentous protein network of TPR

Beatriz M. A. Fontoura, Samuel Dales, Günter Blobel*, and Hualin Zhong

Laboratory of Cell Biology, Howard Hughes Medical Institute, The Rockefeller University, New York, NY 10021

Contributed by Günter Blobel, January 10, 2001

The Nup98 gene codes for several alternatively spliced protein precursors. Two *in vitro* translated and autoproteolytically cleaved precursors yielded heterodimers of Nup98-6kDa peptide and Nup98-Nup96. TPR (translocated promoter region) is a protein that forms filamentous structures extending from nuclear pore complexes (NPCs) to intranuclear sites. We found that *in vitro* translated TPR bound to *in vitro* translated Nup98 and, via Nup98, to Nup96. Double-immunofluorescence microscopy with antibodies to TPR and Nup98 showed colocalization. In confocal sections the nucleolus itself was only weakly stained but there was intensive perinucleolar staining. Striking spike-like structures emanated from this perinucleolar ring and attenuated into thinner structures as they extended to the nuclear periphery. This characteristic staining pattern of the TPR network was considerably enhanced when a myc-tagged pyruvate kinase-6kDa fusion protein was overexpressed in HeLa cells. Double-immunoelectron microscopy of these cells using anti-myc and anti-TPR antibodies and secondary gold-coupled antibodies yielded row-like arrangements of gold particles. Taken together, the immunolocalization data support previous electron microscopical data, suggesting that TPR forms filaments that extend from the NPC to the nucleolus. We discuss the possible implications of the association of Nup98 with this intranuclear TPR network for an intranuclear phase of transport.

How are macromolecules transported within the crowded interior of the nucleus? Does traffic proceed by simple or by facilitated diffusion, and, if so, what are the structures that might facilitate diffusion?

One of the most intriguing candidate proteins that might participate in the formation of paths for intranuclear diffusion is the large protein, TPR (for translocated promoter region). TPR forms filaments that emanate from the nuclear basket of the nuclear pore complex (NPC) and extend to the nucleolus (1, 2). The full-length mammalian TPR is about 270 kDa. Its amino-terminal region of about 200 kDa predicts a coiled-coil structure that is likely to be involved in filament formation (1, 3–7).

Field-emission scanning electron microscopy of isolated amphibian oocyte nuclear envelopes has revealed striking hollow cables that emanate from the NPC toward the nuclear interior. Interestingly, many of the NPC-attached hollow cables anastomose with each other after projecting only a short distance into the nucleus (8). These ''branching hollow cables'' are most likely formed by TPR, either alone or together with other proteins. In support of the scanning electron microscopy data from amphibian oocytes are immunofluorescence localization studies of TPR in *Drosophila* cells. Here, TPR has been shown to delineate a chromatin-free network that extends from the nuclear envelope to the perinucleolar region (2).

Together these structural and localization data suggest at least two functions for TPR. One is that TPR plays an important role in the organization of interphase chromatin. In support for such a function are recent data on yeast TPR showing that gene deletion disrupts the clustering of perinuclear telomeres and results in a severe deficiency in the repair of DNA double-strand breaks (9). Another function of TPR, synergistic with its chromatin-organizing function, might be to form a chromatin-free passage way to facilitate bidirectional transport between the NPC and the nuclear interior (2, 10).

A great deal has been learned about bidirectional macromolecular transport across the NPC. At least two built-in asymmetries appear to be principal determinants for the vectoriality of transport. One is asymmetric localization of several distinct nucleoporins (Nups) exclusively on one side of the NPC, either its cytoplasmic or its nuclear side (11–17). The other built-in asymmetry is thought to be the predominance of the small GTPase Ran in its GTP-bound form in the nucleoplasm and in its GDP-bound form in the cytoplasm. This asymmetry is due to localization of the Ran GTPase-activating protein 1 (RanGAP1) in the cytoplasm and the Ran GDP/GTP exchange factor (RanGEF or RCC1, regulator of chromatin condensation 1) in the nucleoplasm.

The principal determinants for admission to or exit from the nucleus are sequence elements: nuclear localization sequences (NLSs) for import and nuclear export sequences for export. These sequences are recognized by cognate signal-recognition factors. Because these factors ferry to and from the nucleus and because they belong to a structurally related family of proteins, they have been termed karyopherins (Kaps) (also known as importins, exportins, and transportins). Besides recognizing a cognate NLS or nuclear export sequences, each Kap is able to dock to a subgroup of Nups that contain FG (Phe-Gly) repeats. Each of the Kaps also can bind to RanGTP.

A thermal ratchet model has been proposed for transport into and out of the nucleus (17). For import, a Kap binds to its cognate NLS substrate in the cytoplasm. After docking to FG containing Nups on the cytoplasmic side of the NPC, the binary complex diffuses across the central tube of the NPC, where it can bind to FG containing Nups on the nuclear side of the NPC. These processes would be dictated by low affinity interactions and would be bidirectional. However, interaction of the binary complex with high-affinity binding sites that are represented by asymmetrically localized Nups on the nuclear side of the NPC would disfavor back-diffusion into the cytoplasm. The presence of RanGTP on the nuclear side of NPC would cause binding of RanGTP to the Kap of the binary complex and concomitant displacement of the NLS substrate. What happens thereafter is not clear. The import substrate could reach its final intranuclear destination by simple diffusion, whereas the Kap/RanGTP complex could diffuse back into the cytoplasm, where it could be recycled at the cytoplasmic face of the NPC by RanGTP hydrolysis (18). Alternatively, intranuclear transport of the NLS substrate could continue to be facilitated by intranuclear Kaps

Abbreviations: NPC, nuclear pore complex; Nup, nucleoporin; TPR, translocated promoter region; NLS, nuclear localization signal; FG repeats, Phe-Gly repeats; Kaps, karyopherins; PK, pyruvate kinase.

*To whom reprint requests should be addressed. E-mail: blobel@rockvax.rockefeller.edu.

The publication costs of this article were defrayed in part by page charge payment. This article must therefore be hereby marked "*advertisement*" in accordance with 18 U.S.C. §1734 solely to indicate this fact.

www.pnas.org/cgi/doi/10.1073/pnas.061014698

and Nups until delivery of the substrate to a high affinity, intranuclear target site is completed (19, 20).

A thermal ratchet model also could operate for export (17). An intranuclear facilitated phase of transport may precede transport across the central tube of the NPC. A ternary export complex of a nuclear export sequences containing substrate with its cognate Kap and RanGTP might be assembled within the nucleus. After reversible docking at nucleoplasmic FG nucleoporins, diffusion across the central tube of the NPC, and reversible docking at the cytoplasmic FG Nups, the ternary complex would bind with high affinity to asymmetrically localized Nups on the cytoplasmic side of the NPC. The ternary complex then would be disassembled cooperatively by RanGTP hydrolysis and high-affinity binding to cytoplasmic targets.

Nup98 has been localized previously at the nucleoplasmic side of the NPC and inside the nucleus (15, 21). In addition, we have shown colocalization of Nup96 with TPR in the vicinity of the NPC (16). In this paper, we have investigated whether the two nucleoporins, Nup98 and Nup96, interact with TPR. We found that Nup98 binds to TPR. Nup96's amino-terminal region interacts with Nup98 and, thereby, interacts with TPR via Nup98. We have used overexpression of a fusion protein containing the peptide that mediates interaction between Nup98 and Nup96 and pyruvate kinase and have obtained a striking visualization of the intranuclear TPR network by confocal microscopy. Finally, by double-immunoelectron microscopy we demonstrated colocalization of TPR with Nup98 on elongated intranuclear structures that could represent TPR filaments associated with Nup98.

The presence of TPR-associated intranuclear Nups suggests that there is a Nup- and Kap-mediated intranuclear phase of transport. The possible benefits of Nup- and Kap-facilitated intranuclear transport are discussed.

Materials and Methods

Plasmid Construction. Nup98-6kDa precursor, Nup98-Nup96 precursor, Nup98 (1–863), and Nup96 were cloned into pAlterMAX as described previously (16). The Tpr construct (pT7Tpr) was a generous gift from Larry Gerace (The Scripps Research Institute, La Jolla, CA). All these constructs encode proteins with a myc tag at the N terminus. The myc-tagged PK (pyruvate kinase)-6kDa fusion construct was generated by PCR. An oligonucleotide complementary to the 5′ end of the 6kDa region of the Nup98-6kDa precursor coding sequence containing an *Eco*RI site and an antisense oligonucleotide complementary to the 3′ end of the 6kDa region containing an *Xho*I site were used in the PCR. The amplified PCR product was digested with *Eco*RI and *Xho*I and ligated into the *Eco*RI/*Xho*I sites of the pcDNA1-mycPK (kindly provided by Matthew Michael (University of California, San Diego, CA).

***In Vitro* Binding Assays.** All proteins were translated from *in vitro* transcribed RNA by using a coupled reticulocyte lysate transcription/translation system (Promega), in the presence of [^{35}S]methionine, according to the manufacturer's instructions. Immunoprecipitation reactions were carried out by using 50 μl of *in vitro* translated proteins and 450 μl of TBT buffer (20 mM Hepes, pH 7.4/110 mM KOAc/2 mM $MgCl_2$/0.1% Tween 20) with complete EDTA-free protease inhibitors mixture tablet (Roche, Gipf-Oberfrick, Switzerland). In the studies involving protein–protein interaction, 50-μl aliquots of each translation were mixed for 30 min at room temperature and incubated with specific antibodies (as described in the figure legends) diluted in 400 μl of TBT for 1 h at 4°C. The anti-Nup98 and anti-Nup96 polyclonal antibodies have been characterized previously (15, 16). The anti-myc antibodies (A-14) were obtained from Santa Cruz Biotechnology. Reactions then were incubated with 10 μl of protein A-Sepharose CL-4B beads (Amersham Pharmacia) for 1 h at 4°C. The precipitated pellets were washed four times with TBT buffer and resuspended in 30 μl of SDS-sample buffer. The immunoprecipitated proteins were separated by SDS/PAGE (NOVEX, San Diego) and analyzed by autoradiography.

Immunofluorescence and Confocal Microscopy. Immunofluorescence microscopy using HeLa cells was performed as described previously (16). The anti-Nup98 polyclonal antibodies (15) were affinity-purified as reported (22) and diluted 1:10. The anti-Tpr mAb 5E10 (kindly provided by Michael Matunis, The Johns Hopkins University, Baltimore, MD) was diluted 1:250. The anti-Nup358 polyclonal antibodies (11) were diluted 1:2,000. Fluorescein-conjugated donkey anti-mouse antibodies (diluted 1:70) and Cy3-conjugated donkey anti-rabbit antibodies (diluted 1:150) were used as secondary antibodies (Jackson ImmunoResearch). The myc-tagged PK-6kDa expression vector was transfected into HeLa cells as described previously (16), and the protein was detected with the anti-myc mAb 9E10 (Boehringer Mannheim) diluted 1:40. Cy3-conjugated donkey anti-mouse antibodies (diluted 1:150) were used as secondary antibodies (Jackson ImmunoResearch). Samples were analyzed by generating optical sections in the *z* axis with a Leica TCS SP spectral confocal microscope.

Immunogold Electron Microscopy. One 10-cm Petri dish of HeLa cells transfected with the myc-PK-6kDa expression vector was washed with ice-cold PBS. Cells were harvested with cold TEA buffer containing 20 mM triethanolamine, pH 7.5, 100 mM NaCl, 2 mM MgCl2, 0.5 mM CaCl2, 1 mM DTT, 0.5 mM PMSF, 1 μg/ml leupeptin, 1 μg/ml pepstatin A, and 18 μg/ml aprotinin. Cells were broken in a Dounce homogenizer. Nuclei were centrifuged at 800 $\times$ *g* for 5 min at 4°C, resuspended in TEA buffer, and incubated with 10 μg/ml DNase I (Sigma) and 10 μg/ml RNase A (Sigma) for 10 min at 20°C. The digested nuclei were centrifuged at 800 $\times$ *g* for 5 min at 4°C, resuspended in TEA buffer, and then centrifuged at 3,000 $\times$ *g* for 3 min at 4°C. The pellet was fixed with 2% formaldehyde and 0.1% glutaraldehyde in TEA buffer for 15 min, washed with TEA buffer, and dehydrated by increasing concentrations (30–100%) of *N*,*N*-dimethylformamide (DMF) (Aldrich). The pellet was embedded in Lowicryl K4M resin (Lowi, Waldkralburg, Germany) and then immersed in DMF/K4M (1:1) for 1 h and K4M at −20°C for 8 h. The resin was polymerized under UV light at −20°C for 3 h. Sections of ≈80–100 nm in thickness were mounted on nickel grids coated by a film of formvar–carbon and reacted with the rabbit anti-myc antibodies (A-14) for detection of the myc-PK-6kDa fusion protein and the mouse anti-Tpr mAb 5E10. Rabbit antibodies were detected with 5-nm gold-coupled secondary antibodies, whereas mouse antibodies were detected with 10-nm gold-conjugated secondary antibodies (Amersham Pharmacia) and stained with aqueous uranyl acetate. Samples were examined in a JEOL 100 CX electron microscope at 80 kV.

Results

The Autoproteolytic Fragments of Two Nup98 Precursors Remain Associated. The Nup98 gene gives rise to several alternatively spliced precursor proteins (16, 23). Two of the alternatively spliced mRNAs produce a Nup98-6kDa precursor and a Nup98-Nup96 precursor (see Fig. 1*A*). An unusual feature of these precursors is that they contain a site for proteolysis. Cleavage is not by a protease but by an autoproteolytic mechanism (24). Interestingly, when recombinant proteins containing up- and downstream regions of the cleavage site are expressed in *Escherichia coli*, the two autoproteolytic fragments remain noncovalently linked to each other (24).

To determine whether the autoproteolytic cleavage products of the two Nup98 precursors (see Fig. 1*A*) associate with each other, *in vitro* transcribed mRNAs that code for various Nup98

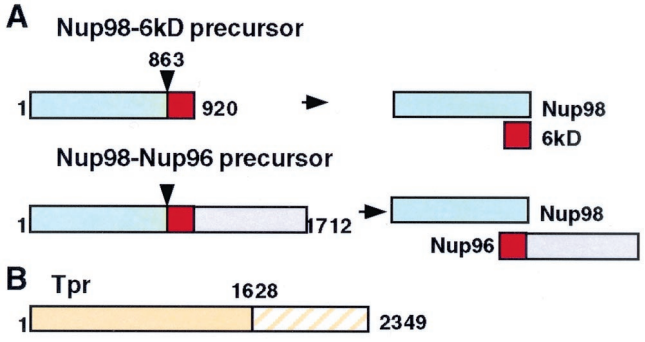

Fig. 1. Schematic representation of two Nup98 precursor proteins and TPR. Two alternatively spliced mRNAs of the Nup98 gene code for a Nup98-6kDa and Nup98-Nup96 precursor, both of them autoproteolytically cleaved at residue 863. The cleaved products remain associated with each other. Because of alternative splicing, the 6kDa region of Nup96 (indicated in red) lacks six carboxyl-terminal residues that are present in the 6kDa peptide of the Nup98-6kDa precursor. TPR contains an amino-terminal region of 1,628 residues that is likely to form a coiled coil, whereas the carboxyl-terminal remainder is highly charged.

precursors with an amino-terminally tagged myc epitope were translated in the reticulocyte lysate system. We used anti-myc antibodies for immunoprecipitation and SDS/PAGE and autoradiography for subsequent analysis of the immunoprecipitate (Fig. 2). To detect an autoproteolytically generated 6kDa peptide, we translated two Nup98 mRNAs: one coding for myc-Nup98-6kDa peptide and the other one only for myc-Nup98. In both cases we observed a major protein at the predicted M_r of Nup98 (see arrow, Fig. 2*A*) plus a number of smaller proteins that are likely a result of downstream translation initiation. A distinct, small peptide of an estimated 6kDa was coprecipitated with anti-myc antibodies from the translation products of myc-Nup98-6kDa (Fig. 2*A*, lane 1). Such a peptide was absent from the translation products of a myc-Nup98 mRNA that lacked the region coding for the 6kDa peptide (Fig. 2*A*, lane 2). These data

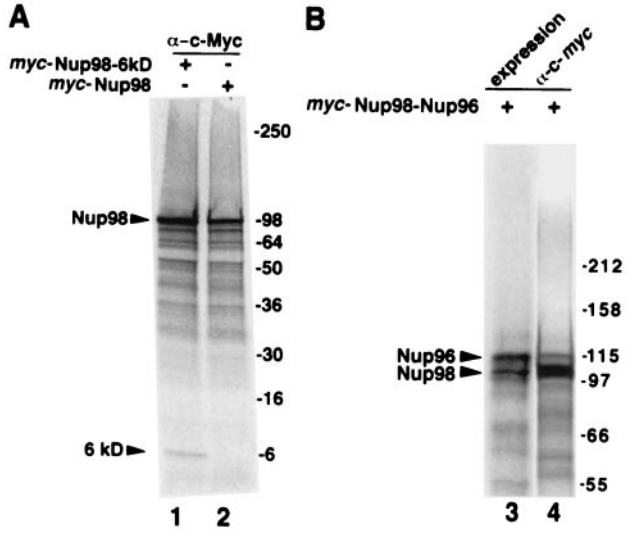

Fig. 2. The autoproteolyzed products of Nup98-6kDa and Nup98-Nup96 remain associated with each other. Several mRNAs coding for myc-tagged Nup98 variants were translated in a reticulocyte lysate system. Total translation products (lane 3, expression) or immunoprecipitates of translation products with anti-myc antibodies (lanes 1, 2, and 4) were analyzed by SDS/PAGE (4–20% in *A* and 8% in *B*) and autoradiography.

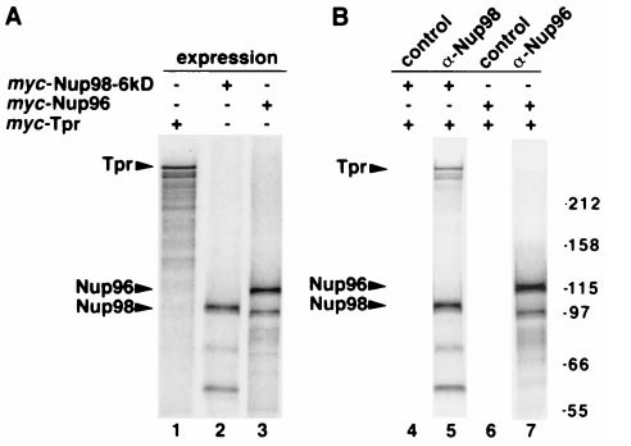

Fig. 3. TPR binds to Nup98 but not to Nup96. Several mRNAs coding for myc-tagged TPR or indicated Nup98 variants were translated separately in a reticulocyte lysate system. As indicated, aliquots were analyzed either directly (expression) or after posttranslational incubation and immunoprecipitation with the indicated antibodies (anti-Nup98 or anti-Nup96) or mock-immunoprecipitation in the absence of antibodies (control). Analysis was by SDS/PAGE and autoradiography.

strongly suggest that the 6kDa fragment of the Nup98-6kDa precursor remains associated with Nup98.

Likewise, Nup96 resulting from proteolysis of a myc-Nup98-Nup96 precursor (Fig. 2*B*, lane 3) remained associated with Nup98 (Fig. 2*B*, lane 4). However, not all of the Nup96 was recovered in the immunoprecipitate (Fig. 2*B*, lanes 3 and 4). It is presently not clear why only a fraction of Nup96 remains associated with Nup98 (see *Discussion*).

Nup98, but Not Nup96, Interacts with TPR. To determine whether TPR interacts with Nup98 and/or Nup96, we translated *in vitro* transcribed mRNAs coding for myc-Nup98-6kDa, myc-Nup96, or myc-TPR in the reticulocyte lysate (Fig. 3*A*). In each case we obtained a major band that likely represents the corresponding full length translation product (Fig. 3*A*). After posttranslational incubation of various translations, we carried out immunoprecipitation with anti-Nup98- or anti-Nup96-specific antibodies and analyzed the immunoprecipitates by SDS/PAGE and autoradiography (Fig. 3). We found that TPR interacted with Nup98 as posttranslational incubation of TPR and Nup98 and subsequent immunoprecipitation with anti-Nup98 antibodies coprecipitated TPR (Fig. 3*B*, lanes 4 and 5). In contrast, Nup96 did not interact with TPR. Posttranslational incubation of Nup96 with TPR and subsequent immunoprecipitation with anti-Nup96 antibodies did not coprecipitate TPR (Fig. 3*B*, lanes 6 and 7).

Nup96 Interacts Indirectly with TPR via Nup98. Because Nup96 and Nup98 interact with each other, it is likely that Nup96 might indirectly interact with TPR, via Nup98. Indeed, posttranslational incubation of TPR with Nup98-Nup96 and subsequent immunoprecipitation with anti-Nup96 antibodies coprecipitated TPR (Fig. 4*A*, compare lanes 1 and 2). Together with the results shown in Fig. 3*B*, lane 7, these data suggest that Nup96 does not interact directly with TPR but interacts indirectly, via Nup98.

The 6kDa Peptide Does Not Mediate Binding to TPR. To determine whether the 6kDa peptide region is involved in binding to TPR, we incubated translations containing TPR and either Nup98 or Nup98-6kDa and immunoprecipitated with anti-Nup98 antibodies. In both cases TPR was coprecipitated (Fig. 4*B*, lanes 3 and 4), indicating that the 6kDa region is not involved in mediating interaction of Nup98 with TPR. Taken together, we conclude

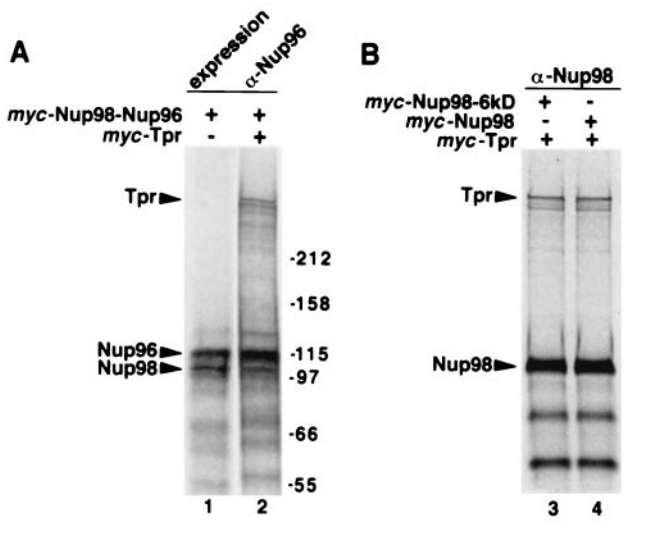

Fig. 4. Nup96 binds to TPR indirectly via Nup98. Several mRNAs coding for myc-tagged TPR or Nup98 variants were translated separately in a reticulocyte lysate system. As indicated, aliquots were analyzed either directly (expression) or after posttranslational incubation and immunoprecipitation with the indicated antibodies. Analysis was by SDS/PAGE and autoradiography.

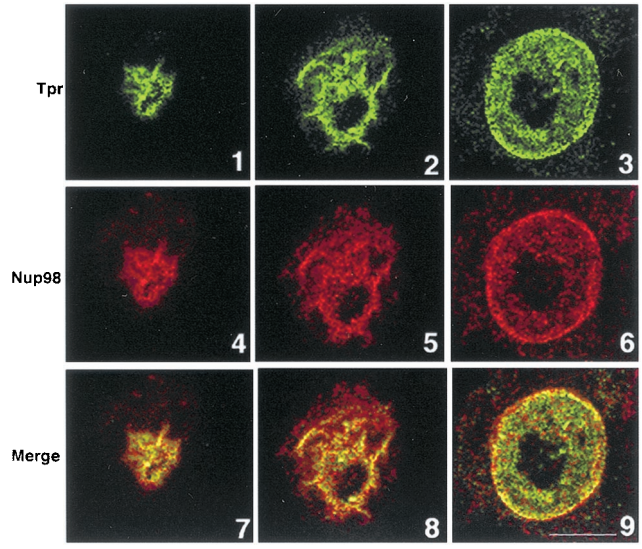

Fig. 6. Colocalization of TPR and Nup98 in an intranuclear network and at the nuclear periphery. HeLa cells were fixed, permeabilized, and incubated with anti-TPR or anti-Nup98 antibodies for double-immunofluorescence analysis by confocal microscopy. Shown are 3 of 32 optical sections across the HeLa cell nucleus in the *z* axis. Sections 1, 4, and 7 are in a plane above the nucleolus. Sections 2, 5, and 8 are through one pole of the nucleolus; note perinucleolar labeling and spikes that attenuate as they project into the nuclear periphery. Sections 3, 6, and 9 are near equatorial sections through the nucleus; note punctate labeling in the nucleus and the nuclear periphery. (Bar = 10 μm.)

(see model in Fig. 5) that Nup98 binds to TPR and that the 6kDa region mediates the binding of Nup98 with Nup96 and, hence, the indirect interaction of Nup96 with TPR.

TPR Colocalizes with Nup98 in the Nuclear Interior. To corroborate the binding results by *in situ* localization data, we carried out double-immunofluorescence confocal microscopy on HeLa cells. We used a mouse monoclonal anti-TPR antibody. The epitope of TPR that reacts with the mAb has not yet been defined. We also used rabbit polyclonal antibodies that were raised against recombinant Nup98 (15). Several representative confocal sections in the *z* axis are shown in Fig. 6. One set of sections (Fig. 6, sections 1, 4, and 7) shows intense staining on the surface of the nucleolus where both TPR and Nup98 colocalize. Particularly striking are spike-like structures that emanate from the nucleolus and become thinner as they project toward the nuclear periphery. Again, these structures are stained by both anti-Nup98 and anti-TPR antibodies. Finally, in a near-equatorial section (sections 3, 6, and 9) a finely punctate staining of the nuclear interior and the nuclear periphery is visible. There is partial but not complete overlap of TPR with Nup98. The reason for an incomplete overlap may be that TPR is a long, filamentous molecule. Only a portion of it would be decorated by the mAbs whereas Nup98 would be globally decorated by the polyclonal anti-Nup98 antibodies.

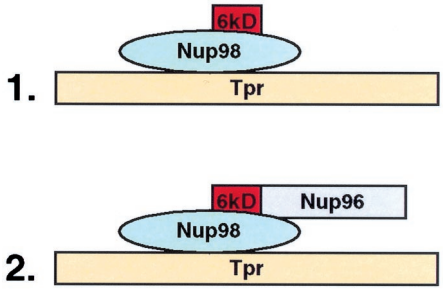

Fig. 5. Summary model of binding data. Nup98 binds to TPR, and Nup96 binds indirectly via its amino-terminal region.

Decoration of the TPR Network by Overexpression of a Fusion Protein That Contains the 6kDa Region. We transiently transfected HeLa cells with constructs that coded for two distinct fusion proteins, either myc-PK or myc-PK-6kDa. As expected, the myc-PK fusion protein lacking an NLS remained in the cytoplasm (Fig. 7*A*). However, the myc-PK-6kDa fusion protein was localized to the nucleus, indicating that the 6kDa region contributes an NLS. This was surprising, because our previous data using transient transfection with a construct coding for a myc-Nup96 fusion protein showed that this fusion protein was located in the cytoplasm. Hence, it appears that the 6kDa region contains an NLS. This NLS appears to be masked when the 6kDa region is part of Nup96. Double-immunofluorescence with polyclonal antibodies to Nup358, a cytoplasmically exposed nucleoporin (11, 12), and anti-myc antibodies showed that the myc-PK-6kDa fusion protein is clearly within the nucleus (Fig. 7*B*, section 1). Confocal sections from the surface of the nucleolus (section 2) across the center of the nucleolus (sections 3–6) show a staining pattern that is essentially similar to that shown in Fig. 6 for TPR and Nup98. The center of the nucleolus is weakly stained (sections 3–6). There is an intense, ring-like staining around the nucleolus (sections 3–5) with prominent spikes emanating from this perinucleolar ring. Again, these spikes become thinner as they extend into the nuclear periphery. These data suggest that the 6kDa region of this fusion protein was able to displace either the endogenous 6kDa region of Nup98-6kDa or endogenous Nup96 that contains the amino-terminal 6kDa region. The fusion protein is likely to form a tetramer via PK. This may have led to an enhancement of the immunofluorescence signal.

To further sublocalize the myc-PK-6kDa fusion protein relative to TPR, we carried out double-immunoelectron microscopy by using mouse mAb against TPR (10-nm gold) and anti-myc antibodies (5-nm gold) (Fig. 8). Many regions of colabeling can be found with gold particles of both types decorating tracks often more than 100 nm in length. These data extend and corroborate the binding results and the immunofluorescence data.

CELL BIOLOGY

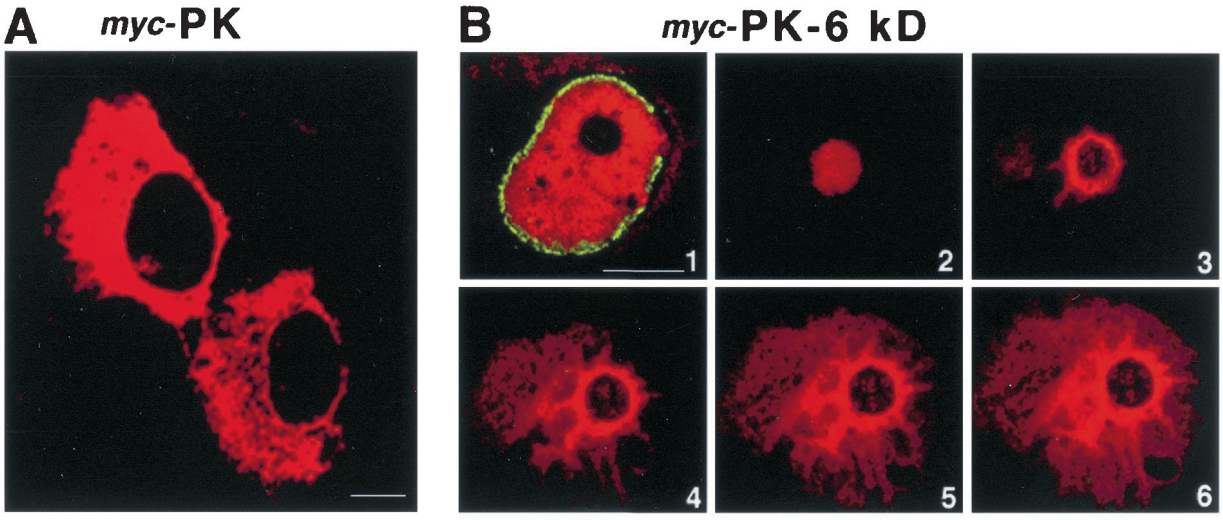

Fig. 7. Immunofluorescence visualization of the TPR network is enhanced by overexpression of a myc-PK-6kDa construct. HeLa cells were transiently transfected with a myc-PK or a myc-PK-6kDa construct. Note that the myc-PK fusion protein is excluded from the nucleus (*A*), whereas the myc-PK-6kDa fusion protein gains access to the nucleus (*B*, 1–6). In *B*, cells were prepared for double-immunofluorescence with anti-Nup358 antibodies and anti-myc antibodies. Six of 64 confocal nuclear sections are shown: an equatorial nuclear section, *B*1, demonstrates Nup358 staining in green at the cytoplasmic side of the nuclear envelope and the intranuclear staining of myc-PK-6kDa in red. Sections above the nucleolus (*B*2) and across the nucleolus (*B*3–6) show the characteristic but much enhanced features of TPR and Nup98 labeling seen in Fig. 6: intense staining of the perinucleolar region from which spikes emanate and attenuate as they project into the nuclear periphery. (Bar = 10 μm.)

Discussion

Our data here show that the nucleoporin Nup98 interacts with the entire filamentous TPR network that extends from the nuclear periphery on the nucleoplasmic side of the NPC to the interior of the nucleus and terminates at the nucleolus. Nup96 interacts indirectly with TPR via Nup98. Although the function of Nup96 is unknown, Nup98, as an FG repeat nucleoporin, has been shown to bind directly to karyopherin β2 as well as Ran GDP/GTP exchange factor (25). The association of Nup98 with TPR provides strong evidence for Nup- and Kap-facilitated intranuclear transport along TPR filaments.

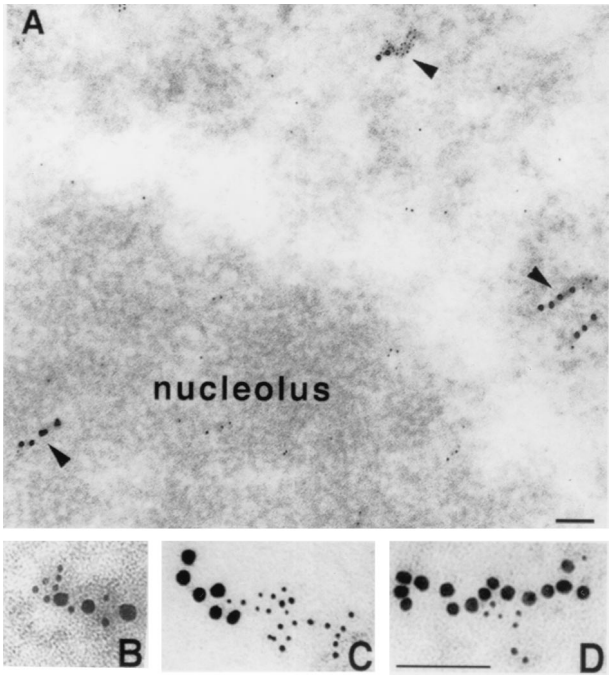

Fig. 8. Colocalization of TPR and the myc-PK-6kDa fusion protein. HeLa cells were transiently transfected with the myc-PK-6kDa construct and prepared for double-immunoelectron microscopy. The 10-nm gold particles represent TPR, and the 5-nm gold particles represent the myc-PK-6kDa fusion protein. Note the colocalization of particles in rows. (Bar = 100 nm.)

The Nup98 gene consists of 31 exons. Northern blots suggest the existence of at least four distinct mRNAs (16). These mRNAs appear to code for precursor proteins that are processed autoproteolytically at one distinct site (refs. 16, 23, and 24; see Fig. 1). The products of three mRNAs have been characterized. The largest and most abundant of these mRNAs is likely to code for the Nup98-Nup96 precursor, whereas the smallest and least abundant mRNA is likely to code for the Nup98-6kDa precursor (16) (see Fig. 1). The cleavage products of these two precursors remain associated with each other (ref. 24; Fig. 2). Hence, *in vivo* these two mRNAs give rise to two Nup98 species: a minor one that is associated with a 6kDa peptide and an abundant one that is associated with Nup96. It is likely that Nup98-bound 6kDa peptide or Nup96 differentiates the function of Nup98. It remains to be investigated whether the two Nup98 complexes differ in their intranuclear localization (e.g., NPC vs. intranuclear localization).

We noticed that not all of the *in vitro* translated Nup96 derived from the Nup98-Nup96 precursor remains associated with Nup98 (Fig. 2*B*). One possible reason is that distinct phosphorylation sites that are present in the 6kDa region are phosphorylated differentially by kinases in the reticulocyte lysate and that this might affect the degree of association.

In agreement with the biochemical binding data, we found by double-immunofluorescence microscopy that Nup98 and TPR colocalized. In confocal sections, TPR and Nup98 were found in a perinucleolar region with weak labeling present inside the nucleolus (Fig. 6). From the perinucleolar region, the colocalization of Nup98 and TPR proceeded along spikes (Fig. 6, sections 2, 5, and 8) that attenuated as they extended toward the nuclear periphery. There, the colocalization of TPR and Nup98 yielded the characteristic punctate staining of NPCs and subjacent nuclear regions (Fig. 6, sections 3, 6, and 9).

Particularly striking immunofluorescence images were obtained from cells that were transfected with a myc-PK-6kDa fusion protein and then probed with anti-myc antibodies. The tetramerization of the PK moiety of this fusion protein is likely responsible for an amplification of the fluorescence signal. Via an apparent NLS in the 6kDa region, this fusion protein was imported into the nucleus, where it likely interacted with Nup98 bound to TPR, perhaps displacing endogenous 6kDa peptide or endogenous Nup96. This resulted in an extensive staining of the TPR network in the form of an intense perinucleolar ring and attenuating spikes that extended from this perinucleolar ring to the nuclear periphery (Fig. 7*B*, sections 3–6). Taken together, these immunofluorescence data are entirely consistent with the proposed existence of filaments that originate at the NPC and then merge and converge at the perinucleolar region (1, 2). Our data strongly suggest that these structures contain TPR and Nup98 and indirectly bound Nup96.

Double-immunoelectron microscopy confirmed the colocalization of TPR and Nup98 in the nuclear interior with the respective immunogold particles aligned in rows of several particles, consistent with the filamentous structure of TPR (Fig. 8). Track-like immunogold decorations extending between the nucleolus and the NPC have been described previously for a protein (Nopp140) that shuttles between the nucleolus and the cytoplasm. In favorable sections, curvilinear tracks of gold particles could be detected to extend over several microns in length (26). It is likely that these tracks represent transport substrate (Nopp140) transported on TPR filaments between the nucleolus and across the NPC into the cytoplasm.

TPR is a huge molecule with potentially many binding sites. The interaction of Nup98 with TPR most likely is a direct one, although we cannot presently rule out that a protein of the reticulocyte lysate mediated this interaction. The mutual binding epitopes of Nup98 and TPR remain to be mapped. Nup153 has been shown previously by immunoelectron microscopy to be located at the nucleoplasmic side of NPC and in the nuclear interior (14, 27). If TPR, in addition to Nup98, also binds Nup153 and perhaps other not-yet-identified nucleoporins of the nucleoplasmic side of the NPC, the TPR network with its associated Nups could be considered an intranuclear extension of the nucleoplasmic aspect of the NPC. Import of substrates to their proper intranuclear sites and export from intranuclear sites would have a distinct intranuclear phase. For both import and export, a Kap- and Nup-mediated intranuclear phase of transport would take advantage of the chaperoning function of the Kaps and would allow a stepwise and coordinated assembly of large intranuclear complexes. For example, for import, it might facilitate the stepwise and coordinated assembly at predestined intranuclear sites of the many large complexes that operate in the nucleus. These may include the abundant histone octamers and other large complexes that function within the nucleus in transcription, splicing, DNA replication, DNA repair, chromosome remodeling, and cell cycle regulation, to name a few examples. Moreover, complexes that ultimately are destined for export, such as ribosomal subunits and mRNPs, could be assembled by these mechanisms within the nucleus in a coordinated and stepwise fashion. After their birth on cytoplasmic ribosomes, individual proteins or posttranslationally assembled subcomplexes each would react with their cognate Kaps. These complexes would be transported across the NPC and then along the TPR network within the nucleus. Once the substrate/Kap complex arrives at its intranuclear target, the substrate would be cooperatively and irreversibly dissociated from the Kap by high-affinity binding to an already localized intranuclear constituent and by RanGTP. Facilitated transport and cooperative disassembly of transport complexes would yield targeted delivery and stepwise and coordinated intranuclear assembly of these complexes (19, 20). Similar scenarios can be envisaged for the stepwise intranuclear disassembly of large intranuclear complexes and the subsequent facilitated export of disassembled constituents along the TPR network and across the NPC.

We thank E. Ellison for technical assistance, M. Matunis and L. Gerace for helpful reagents, and V. Nussenzweig for critical reading of the manuscript.

1. Cordes, V. C., Reidenbach, S., Rackwitz, H. R. & Franke, W. W. (1997) *J. Cell. Biol.* **136,** 515–529.
2. Zimowska, G., Aris, J. P. & Paddy, M. R. (1997) *J. Cell. Sci.* **110,** 927–944.
3. Park, M., Dean, M., Cooper, C. S., Schmidt, M., O'Brien, S. J., Blair, D. G. & Vande Woude, G. F. (1986) *Cell* **45,** 895–904.
4. Mitchell, P. J. & Cooper, C. S. (1992) *Oncogene* **7,** 2329–2333.
5. Byrd, D. A., Sweet, D. J., Pante, N., Konstantinov, K. N., Guan, T., Saphire, A. C., Mitchell, P. J., Cooper, C. S., Aebi, U. & Gerace, L. (1994) *J. Cell. Biol.* **127,** 1515–1526.
6. Bangs, P. L., Sparks, C. A., Odgren, P. R. & Fey, E. G. (1996) *J. Cell. Biochem.* **61,** 48–60.
7. Kosova, B., Pante, N., Rollenhagen, C., Podtelejnikov, A., Mann, M., Aebi, U. & Hurt, E. (2000) *J. Biol. Chem.* **275,** 343–350.
8. Ris, H. (1997) *Scanning* **19,** 368–375.
9. Galy, V., Olivo-Marin, J. C., Scherthan, H., Doye, V., Rascalou, N. & Nehrbass, U. (2000) *Nature (London)* **403,** 108–112.
10. Paddy, M. R. (1998) *Am. J. Hum. Genet.* **63,** 305–310.
11. Wu, J., Matunis, M. J., Kraemer, D., Blobel, G. & Coutavas, E. (1995) *J. Biol. Chem.* **270,** 14209–14213.
12. Yokoyama, N., Hayashi, N., Seki, T., Pante, N., Ohba, T., Nishii, K., Kuma, K., Hayashida, T., Miyata, T., Aebi, U., *et al.* (1995) *Nature (London)* **376,** 184–188.
13. Kraemer, D., Wozniak, R. W., Blobel, G. & Radu, A. (1994) *Proc. Natl. Acad. Sci. USA* **91,** 1519–1523.
14. Sukegawa, J. & Blobel, G. (1993) *Cell* **72,** 29–38.
15. Radu, A., Moore, M. S. & Blobel, G. (1995) *Cell* **81,** 215–222.
16. Fontoura, B. M., Blobel, G. & Matunis, M. J. (1999) *J. Cell. Biol.* **144,** 1097–1112.
17. Rout, M., D., Aitchison, J., Suprapto, A., Hjertaas, K., Zhao, Y. & Chait, B. T. (2000) *J. Cell. Biol.* **148,** 635–651.
18. Yaseen, N. R. & Blobel, G. (1999) *J. Biol. Chem.* **274,** 26493–26502.
19. Pemberton, L. F., Rosenblum, J. S. & Blobel, G. (1999) *J. Cell. Biol.* **145,** 1407–1417.
20. Lee, D. C. & Aitchison, J. (1999) *J. Biol. Chem.* **274,** 29031–29037.
21. Powers, M. A., Macaulay, C., Masiarz, F. R. & Forbes, D. J. (1995) *J. Cell. Biol.* **128,** 721–736.
22. Drenckhahn, D. & Franz, H. (1986) *J. Cell. Biol.* **102,** 1843–1852.
23. Kasper, L. H., Brindle, P. K., Schnabel, C. A., Pritchard, C. E., Cleary, M. L. & van Deursen, J. M. (1999) *Mol. Cell. Biol.* **19,** 764–776.
24. Rosenblum, J. S. & Blobel, G. (1999) *Proc. Natl. Acad. Sci. USA* **96,** 11370–11375.
25. Fontoura, B. M., Blobel, G. & Yaseen, N. R. (2000) *J. Biol. Chem.* **275,** 31289–31296.
26. Meier, U. T. & Blobel, G. (1992) *Cell* **70,** 127–138.
27. Cordes, V. C., Reidenbach, S., Kohler, A., Stuurman, N., van Driel, R. & Franke, W. W. (1993) *J. Cell. Biol.* **123,** 1333–1344.